*35th EPS Conference on Plasma Phys. Hersonissos, 9 - 13 June 2008 ECA Vol.**32D**, P-2.062 (2008)*

Investigation of Wendelstein 7-X Configurations with Increased Toroidal Mirror

J. Geiger, H. Maassberg, C. D. Beidler
Max-Planck-Institut für Plasmaphysik, IPP-EURATOM Association, Greifswald, Germany

1. Introduction

The magnetic coil system of Wendelstein 7-X is the result of an optimization procedure concerned with the physics properties of a magnetic configuration important for a fusion reactor, such as equilibrium, stability, neoclassical transport and α-particle confinement [1]. The optimization led to a 5 field period HELIcal-axis-Advanced-Stellarator HELIAS configuration with reduced equilibrium and bootstrap currents. Good α-particle confinement required a toroidal mirror of 10% and was also beneficial for further reduction of the bootstrap current. The mirror ratio is defined as $(B_{\varphi=0}-B_{\varphi=36})/(B_{\varphi=0}+B_{\varphi=36})$, φ=0, 36 being the toroidal angles of the two symmetry planes. Major resonances are avoided by a rather flat profile of the rotational transform ι with a central value above 5/6 and below 1 at the boundary. A vacuum magnetic well of 1% together with the finite shear in the outer half of the plasma provides MHD-stability up to $<\beta>$-values of 5%. The configuration was realised with 10 modular coils per field period. For experimental flexibility, the currents in the modular coil system can be adjusted independently, so that the toroidal mirror can be varied to influence size, location and behavior of the trapped particle population. An additional 4 planar coils per period allow the adjustment of rotational transform and plasma position. Reference cases have been proposed at the beginning of the project [2,3] to show the flexibility regarding rotational transform (low- ι_a (5/6), standard (5/5), high- ι_a (5/4)), shear (low-shear), toroidal mirror term (high- (10%) and low-mirror (0%) compared to standard (5%)) and plasma position (in- and outward shifted). The optimization point in this set is the high-mirror configuration and the standard configuration is named as such because all modular coils carry the same current (no planar coil currents). However, to date there has been no systematic investigation of the large configuration space offered by the W7-X coil system. Limited work was done on stability [4] and on neoclassical transport for optimizing HELIAS-type configurations [5].

This paper starts to investigate the configuration space by considering configurations with different toroidal mirror fields. First, important properties of the reference cases are summarized with their implications for interchange stability. Next, configurations with very large mirror ratios (ca 20%) are explored with respect to interchange stability and initial results on neoclassical transport properties are reported. The pressure profiles generally used are linear in the toroidal flux. The free-boundary 3D-equilibria were calculated with VMEC2000 [6], the local interchange stability analysis is based on the JMC-code[7] and neoclassical transport coefficients were calculated with the DKES-code [8].

2. Reference cases

The reference cases can be viewed as basic variations of the standard configuration in three directions of the configuration space: mirror-ratio, ι and plasma position. In a simplistic model, the modular coils are used for mirror variation and the planar coils for the variation of ι and plasma position. For simplicity this intuitive view is used here, although it should be noted that position variation effectively varies the mirror field. The low-shear and the limiter case can be interpreted as configurations resulting from combinations of these 3 basic variations. Except for the high- and low- ι cases, all reference cases are located at a boundary-ι_a value just below the 5/5-resonance. Figs 1 and 2 show shear and vacuum magnetic well depth for the different configurations being important quantities for local interchange stability. Note that the shear increases

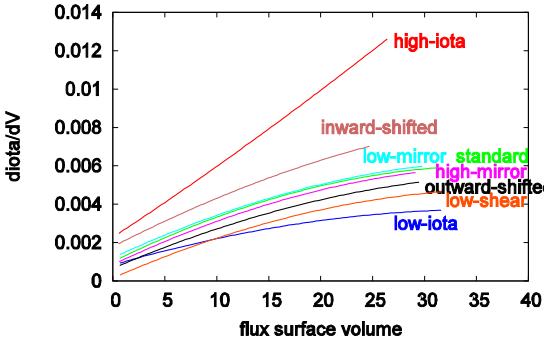

Fig. 1: Shear variation of reference cases.

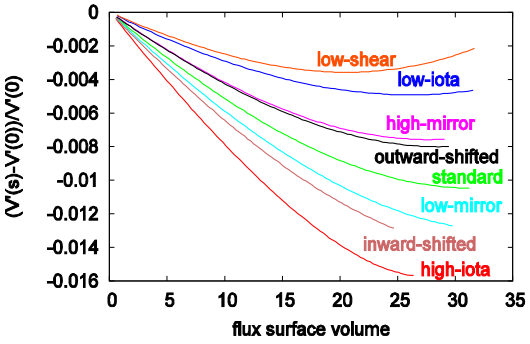

Fig.2: Vacuum magnetic well for reference cases.

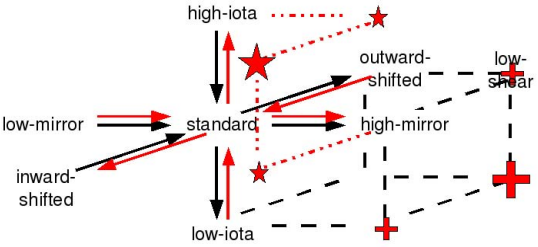

Fig.3: Summary of vacuum configuration changes on shear and magnetic well (black arrows), and on parallel current densities suppression (red arrows). Interesting regions are marked with symbols (stars/crosses).

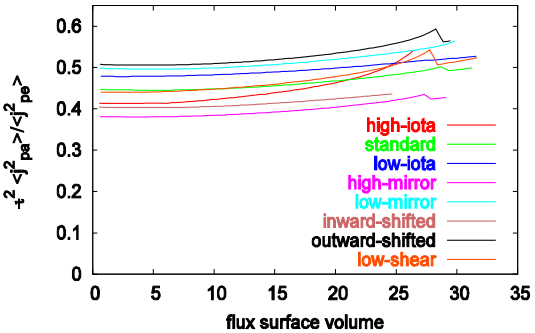

Fig.4: Parallel current density suppression for reference cases. A classical stellarator has a value of 2.

and the magnetic well deepens with ι, with inward-shifting and with a lower mirror-ratio. With respect to inward/outward shifting the effect on the magnetic well is opposite to the situation in LHD where outward shifting deepens the magnetic well. The mirror ratio affects the shear only slightly but affects the vacuum magnetic well depth similar to inward/outward shifting. The joint effect can be seen in the low-shear configuration being a combination of outward-shift and increased mirror field. This is summarized in Fig.3, where black arrows show the trend to less stable configurations. Note that all except the low-shear configuration are Mercier stable for <β>-values up to at least 5-6%, since finite shear acts to stabilise at outer radii where the derivative of V′ is marginal or positive in some cases, e.g. low- ι and high-mirror cases. These configurations already show resistive interchange unstable regions at the boundary for low <β>-values (below 1%).

Another figure of merit to assess configuration properties is the ratio of the average of the square of parallel to perpendicular current density (see [7] for its definition). Since the pressure driven parallel current density is inversely proportional to ι, this dependency can be removed by multiplying the ratio by ι^2. For a classical stellarator this figure of merit can be estimated to be 2. The suppression of the parallel current density by optimization shows up in a reduction of this value. Fig. 4 shows a reduction by roughly a factor of 4 for the reference cases. Within them the ratio falls with increasing ι and mirror-ratio and with inward-shifting. The latter behavior differs from the one observed for shear and vacuum magnetic well. Fig. 3 summarises this with the help of red arrows.

3. Cases with very large toroidal mirror

In a first step the mirror ratio was scanned from slightly inverted (ca -3%) to values twice as large as that of the high-mirror reference case (ca. 23%) without using the planar coils, thus keeping the boundary value of the rotational transform roughly at 5/5. To perform the scan, the two coil currents around the triangular plane (φ=36°) were varied simultaneously while the others were kept constant. The tendency seen with mirror-ratio in the reference cases is also obvious here: with increasing mirror-ratio, the shear is slightly reduced (Fig.5) and the vacuum magnetic well becomes less stabilizing (Fig.6), so that for the largest mirror ratio considered here, a significant vacuum magnetic hill region

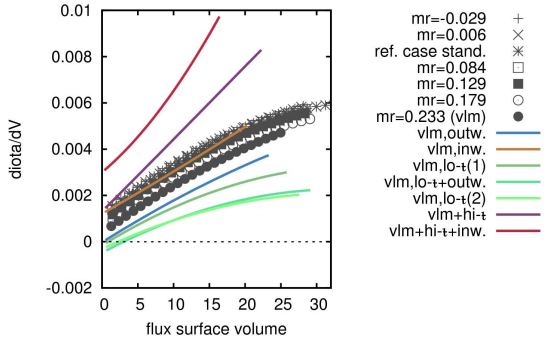

Fig.5: Shear for mirror ratio scan (grey) and variation (color) around the mr=23%-case.

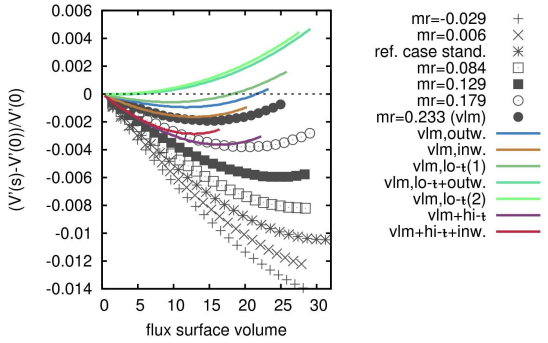

Fig.6: Vacuum magnetic well in mirror scan and variation around the mr=23%-case.

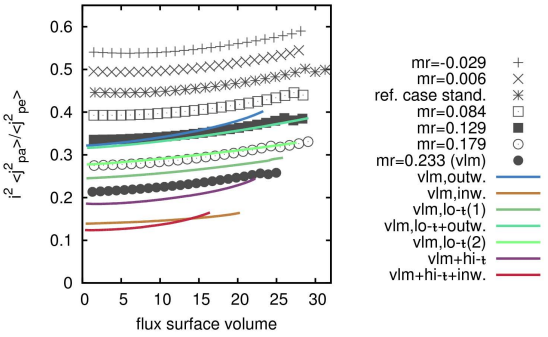

Fig.7: PS-current suppression with mirror ratio and variation around mr=23%-case.

exists in the outer half of the configuration. The parallel current densities show a significant reduction with increasing mirror ratio (Fig. 7). For the very large mirror-case (vlm, ca 23%), the suppression is almost a factor of 2 larger compared to the high-mirror reference case. The interchange stability behavior is dominated by the reduction of the stabilizing shear and vacuum magnetic well. With increasing mirror ratio the configurations become susceptible to interchange modes in the outer half where, as noted, for the highest mirror ratio a vacuum magnetic hill situation develops. For the latter case, ideal stability is maintained at very low β-values due to finite shear, but the outer half becomes unstable to ideal interchange already at moderate <β>-values of 1%. It should be noted, that the volumes of the equilibria have not been adjusted self-consistently to account for possible ergodisation of the boundary.

A variation around the vlm-configuration with a modular field mirror of 23% using the additional planar coils reveals the effect of varying ι and plasma position. The cases are included in Figs 5-7 and can be explained from the tendencies discussed previously. The shortened names used for descriptive purposes refer to the center point for the variation, i.e. the vlm-case. From the variation two classes of interesting configurations emerge. The most unstable configurations result from going to low ι (*vlm,lo-ι(1)* is around 5/6 and *vlm,lo-ι(2)* is below 5/6) possibly in combination with outward-shifting (*vlm,lo-ι-outw.*). In the latter cases, a vacuum magnetic hill region with low shear extends over the entire plasma volume. These configurations are Mercier-unstable from the very beginning with no indication of stabilization with higher β-values. The second class shows a strong suppression of the parallel current density – up to a factor of 3 compared to the standard reference configuration - and arises when shifting inward or when going to high-ι. These configurations show an increased shear and a deeper vacuum magnetic well. They are stable for very low β-values but develop a Mercier-unstable region in the outer half of the plasma volume which grows as β increases. The configurations prove to be very stiff due to the strong reduction of the parallel current densities: very small changes in the ι-profile, no significant Shafranov-shift even at high β. The strong reduction of the parallel currents results from the coupling of the mod-B Fourier harmonics B_{mn} (in Boozer-coordinates) B_{01} (toroidal mirror) and B_{11} (helical) which, for large enough B_{01}, can compete with B_{10} (toroidal curvature term) in the drive of the parallel current densities. A complete suppression of the dipole-part of the secondary currents can be achieved and is especially attractive when combined with good stability and transport properties [9].

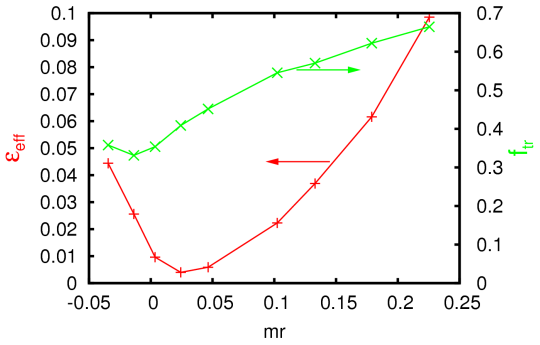

Fig.8: Effective helical ripple and trapped particle fraction for mirror scan.

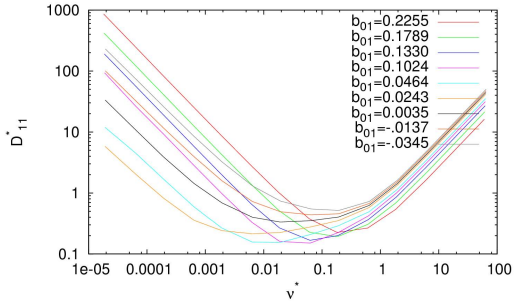

Fig.9: Normalised mono-energetic neoclassical particle transport coefficient for E_r=0 vs normalised collisionality for mirror scan.

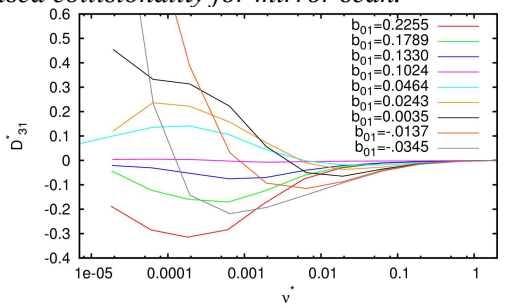

Fig.10: Normalised mono-energetic neoclassical bootstrap current coefficient for E_r=0 vs normalised collisionality for mirror scan.

4. Neoclassical transport

We investigated the neoclassical transport properties at r/a=0.5 and compared the reference configurations with different mirror ratios (mr=0, 4 and 10%) with the large mirror cases (mr=13, 18 and 23%) and added one case between low-mirror and standard configuration and two cases extrapolated to negative mirror ratios. As seen in Fig. 8 from the effective helical ripple, deviation from the optimization points (standard reference case for confinement and high-mirror for bootstrap current suppression) should lead to a significant deoptimisation of the transport properties. For vanishing radial electric field E_r, one observes with increasing mirror that the growing number of trapped particles (Fig.8 for trapped particle fraction) spoils the particle transport coefficient D_{11} (Fig. 9). With inverted mirror, the trapped particles, whose number is slightly growing,is shifted into the regions with increased radial drift velocites resulting in even worse transport properties. Concerning the bootstrap current coefficient (D_{31}), this is minimal for the high-mirror configuration (see Fig. 10) as a result of the optimisation procedure [5]. With increasing mirror, D_{31} becomes negative resulting in an iota-lowering bootstrap current as in quasi-helically symmetric devices, whereas for smaller mirror a tokamak-like bootstrap current evolves. However, for very small or inverted mirror a strong variation of D_{31} is observed which is not yet understood. First investigations on the effect of the radial electric field show an improvement in the particle transport as usually observed. For the bootstrap current, however, the calculations show that part of the optimisation may be lost for medium electric field strengths, leading to values with a sign depending on the toroidal mirror.

References

[1] W. Lotz, J. Nuehrenberg and C. Schwab, *13th Int. Conf. Plasma Physics Control. Nucl. Fus. Res.*, Washington, 1990 (Int. Atomic Energy Agency, Vienna, 1991), Vol. 2, p.603

[2] J. Kisslinger et al., *Proc. 16th Symp. On Fusion Technology*, London 1990 (North Holland Publ., Amsterdam, 1991), Vol.2, 1520-1524

[3] T. Andreeva, IPP-Report, IPP III/270 (2002)

[4] C. Nuehrenberg, Phys. Plasmas **3**, 2401 (1996)

[5] H. Maassberg, W. Lotz and J. Nuehrenberg, Phys. Fluids B **5**, 3728-3736 (1993)

[6] S. Hirshman, W. van Rij and P. Merkel, Comput. Phys. Comm. **43**, 143-155 (1986)

[7] J. Nuehrenberg and R. Zille, in Theory of Fusion Plasmas Varenna 1987 (Editrice Compositori, Bologna, 1988), Vol. EUR 11336 EN, p.3

[8] S. P. Hirshman et al., Phys. Fluids 29, 2951 (1986)

[9] V.R. Bovshuk et al., *34th EPS Conf. on Plasma Phys.*, Warsaw, 2-6 July 2007, P-4.103, http://epsppd.epfl.ch/Warsaw/pdf/P4_103.pdf